15 January 1997

ELSEVIER

Optics Communications 134 (1997) 371–378

OPTICS COMMUNICATIONS

Full length article

Fast fitting of multi-exponential decay curves

Jörg Enderlein [a], Rainer Erdmann [b]

[a] *CST-1, MS M888, Los Alamos National Laboratory, Los Alamos, NM 87545, USA*
[b] *PicoQuant GmbH, Rudower Chaussee 5 (IGZ), 12489 Berlin, Germany*

Received 26 February 1996; revised version received 7 May 1996; accepted 5 June 1996

Abstract

In the analysis of time-resolved measurements of fluorescence decays, one is usually confronted with the essentially non-linear fitting problems. There are several standard methods for non-linear minimisation, but they are all very sensitive to initial guess parameters and are time-consuming. Recently, Sasaki and Masuhara and independently Apanasovich and Novikov proposed an elegant method of quasi-linearising the problem of multi-exponential fitting. In the present paper it will be shown, that their method can be improved by better taking into account the statistical character of the measured data.

1. Introduction

Probing matter with light is one of the most powerful tools for investigating the internal structure and dynamics of molecules and atoms. A special kind of this technique is the excitation of internal electronic states of molecules or atoms by light with wavelengths in the range from the near ultraviolet to the near infrared region. When monitoring the radiating back-transition from the excited levels back to the ground state by detecting the so called fluorescence light, one gets a wealth of information about the nature of excited electronic states [1,2]. Beside the spectral information of the fluorescence light, that means its intensity dependence on excitation and emission wavelengths, an additional measurable parameter is the time characteristic of the fluorescence intensity decay after a strong and short excitation light pulse. The measurement of this decay in time is the subject of the time-resolved fluorescence spectroscopy. For measuring decay times beginning in the range of picoseconds and above, there exist two well established techniques: phase fluorometry and time-correlated single photon counting (TCSPC). In the case of phase fluorometry, the studied probe is excited by an intensity modulated light source, and the fluorescence is detected by a gain modulated detector with the same modulation frequency but shifted modulation phase. By recording the average light intensity in its dependence on the phase shift between excitation intensity modulation and detector gain modulation, the desired decay characteristic of the probe's fluorescence can be extracted. The major drawback of this method is its need for a strong fluorescence signal, anticipating a high concentration of the fluorescing species together with a high fluorescence quantum yield. Contrary to that, the technique of TCSPC does work well even for exceedingly small concentrations of fluorophores and small fluorescence quantum yields [3]. The method consists of exciting the probe by a continuous and periodic train of short light pulses and measuring the arrival time of single fluorescence photons with respect to the time of the last exciting light pulse. By repeating this single photon counting a sufficiently large number of times, a histogram of arrival times is

PII S0030-4018(96)00384-7

built up. The main problem is then to derive the fluorescence decay characteristic with the help of appropriate deconvolution and fitting procedures.

The observed fluorescence intensity $y(t)$ at time t is generally given by

$$y(t) = \int_{-\infty}^{t} \mathrm{d}t'\; x(t-t')K(t'), \tag{1}$$

where $x(t)$ is the time profile of the fluorescence decay of the studied atomic or molecular system, and $K(t)$ is the so called instrumental response function (IRF), containing information about the time profile of the laser excitation and the time characteristics of the whole measurement system. It is assumed, that the excitation of the system is done by an infinite and continuous train of laser pulses so that the integration begins from $t = -\infty$, and $K(t)$ is a periodic function with a period equal to the repetition time of the excitation. Thus, one takes into account also the fluorescence emanating from earlier excitation pulses. This is especially important if one deals with decay times of the order of the repetition time between two excitation pulses.

In general, the measured values of $y(t)$ contain statistical errors, making the inversion of the integral equation (1) an ill-posed problem [4]. For many atomic and molecular systems the excitation and fluorescence process can be described by a simplified quantum-mechanical model including only a finite and discrete number of internal energetic states. In this case, the resulting fluorescence dynamics is characterised by a multi-exponential decay:

$$x(t) = \sum_{i=1}^{M} A_i \exp(-t/\tau_i), \tag{2}$$

where A_i and τ_i are the amplitudes and decay times of the M exponential components of the fluorescence decay. The main purpose of the present paper is to present a fast and straightforward method of fitting such multi-exponential decay curves to experimentally measured fluorescence TCSPC curves.

2. Theory

First of all it should be noted that in practice one deals with discrete numbers of photons y_j in a finite number of time channels $\{t_j - \Delta t/2,\ t_j + \Delta t/2\}$ with centre time t_j and channel width Δt, instead of a continuous function $y(t)$. For sufficiently small channel width Δt, Eq. (1) together with Eq. (2) can then be rewritten as

$$y_k = \sum_{j=0}^{\infty} \sum_{i=1}^{M} A_i \exp(-j\Delta t/\tau_i) K_{k-j}, \tag{3}$$

where y_k and K_k are the number of counts and the instrumental response function value for the kth time channel, respectively. For fitting multi-exponential decay curves to experimental data, many methods of data analysis have been proposed and used in practice, a good overview of which can be found in Ref. [4]. Most frequently, one tries to minimise some error function; the most common used is the least-squares deviation χ^2,

$$\chi^2 = \sum_{k=1}^{N} \frac{\left[y_k - \sum_{j=-\infty}^{k} \sum_{i=1}^{M} A_i \exp(-(k-j)\Delta t/\tau_i) K_j \right]^2}{\sigma_k^2}, \tag{4}$$

where the summation over k runs over all N channels of the TCSPC curve, and the σ_k are the mean square deviations of the photon counts in the kth channel. Since this function depends upon the parameters τ_i in an essentially non-linear way, one normally applies non-linear minimisation methods, like the Nelder–Meade simplex algorithm [5], or the Marquardt–Levenberg method [6,7] for minimising it. Unfortunately, these iteration methods are very sensitive with respect to the initial guess values of the parameters, and can be very time consuming for bad initial guesses, large data sets or larger numbers of exponential components.

Recently, Sasaki and Masuhara [8] proposed a convolved autoregressive model for the fit of multi-exponential decay curves, and independently Apanasovich and Novikov [9] proposed a mathematically equivalent method, the so called Prony's method, for doing this. In both papers, the authors arrived at a quasi-quadratic dependence of the error function upon the fit parameters, allowing the application of the fast and powerful methods of linear least-squares minimisation. But the method of both papers is not accurate enough to be useful in many

cases, especially when one of the decay times is substantially smaller than the range of the TCSPC curve. In the following, an improved implementation of the method is presented and is discussed with respect to a minimisation of the least-squares deviation. But first, the idea of Refs. [8,9] is shortly recalled. The course of reasoning makes use of the so called z-transform, which for an arbitrary series f_i is defined as

$$\tilde{f}(z) = \sum_{i=0}^{\infty} \frac{f_i}{z^i}. \tag{5}$$

Thus, after introducing the abbreviation $z_i = \exp(-\Delta t/\tau_i)$, the z-transform of Eq. (3) yields

$$\tilde{y}(z) = \sum_{i=1}^{M} A_i \tilde{K}(z)(1 - z_i/z)^{-1}. \tag{6}$$

After rearranging Eq. (6) to

$$\tilde{y}(z) \prod_{i=1}^{M}(1 - z_i/z) = \sum_{i=1}^{M} A_i \tilde{K}(z) \prod_{j\neq i}^{M}(1 - z_j/z) \tag{7}$$

and expanding the occurring products into sums (thus defining the new coefficients B_i and C_i),

$$\prod_{i=1}^{M}\left(1 - \frac{z_i}{z}\right) = 1 - \sum_{i=1}^{M} \frac{B_i}{z^i}, \tag{8a}$$

$$\sum_{i=1}^{M} A_i \prod_{j\neq i}^{M}\left(1 - \frac{z_j}{z}\right) = \sum_{i=0}^{M-1} \frac{C_i}{z^i}, \tag{8b}$$

one has

$$\tilde{y}(z) = \sum_{i=1}^{M} \tilde{y}(z) \frac{B_i}{z^i} + \sum_{i=0}^{M-1} \tilde{K}(z) \frac{C_i}{z^i}. \tag{9}$$

Finally, the inverse z-transform gives the desired autoregressive convolution:

$$y_k = \sum_{i=1}^{M} B_i y_{k-i} + \sum_{i=0}^{M-1} C_i K_{k-i}. \tag{10}$$

In vectorial form, this result can be written in especially compact form:

$$\boldsymbol{y} = \hat{D}\boldsymbol{p}, \tag{11}$$

with

$$\boldsymbol{y} = [\, y_{M+1},\ y_{M+2}, \ldots, y_N \,]^{\mathrm{t}}, \tag{12a}$$

$$\boldsymbol{p} = [\, B_1,\ B_2, \ldots, B_M,\ C_0,\ C_1, \ldots, C_{M-1} \,]^{\mathrm{t}}, \tag{12b}$$

$$\hat{D} = \begin{bmatrix} y_M & y_{M-1} & \cdots & y_1 & K_{M+1} & K_M & \cdots & K_2 \\ y_{M+1} & y_M & \cdots & y_2 & K_{M+2} & K_{M+1} & \cdots & K_3 \\ \vdots & \vdots & \cdots & \vdots & \vdots & \vdots & \cdots & \vdots \\ y_{N-1} & y_{N-2} & \cdots & y_{N-M} & K_N & K_{N-1} & \cdots & K_{N-M+1} \end{bmatrix}, \tag{12c}$$

the superscript t denoting transposition, and the finite number N of available measured data points y_i was taken into account.

The big advantage of Eq. (10) is that it is an overdetermined but *linear* system of equations for the unknown parameters C_i and B_i, whereby one has to remember that the known data y_i are subject to statistical error. The authors of Refs. [8,9] are thus looking for a solution for the unknown parameters which is minimising the quadratic form

$$\left(\boldsymbol{y} - \hat{D}\boldsymbol{p}\right)^{\mathrm{t}}\left(\boldsymbol{y} - \hat{D}\boldsymbol{p}\right), \tag{13}$$

leading to the solution

$$\boldsymbol{p} = \left(\hat{D}^{\mathrm{t}}\hat{D}\right)^{-1}\hat{D}^{\mathrm{t}}\boldsymbol{y}. \tag{14}$$

This can be seen by setting the variation of the quadratic form, Eq. (13), after the parameters $\boldsymbol{p}$ to zero,

$$\delta\left[\left(\boldsymbol{y} - \hat{D}\boldsymbol{p}\right)^{\mathrm{t}}\left(\boldsymbol{y} - \hat{D}\boldsymbol{p}\right)\right] = -2\left(\boldsymbol{y} - \hat{D}\boldsymbol{p}\right)^{\mathrm{t}}\hat{D}\ \delta\boldsymbol{p} = 0, \tag{15}$$

which directly leads to Eq. (14). The fact that the second-order variation of Eq. (13) after $\boldsymbol{p}$ is always positive guarantees that the found parameter vector $\boldsymbol{p}$ is indeed minimising the quadratic form (and not maximising it):

$$\delta^2\left[\left(\boldsymbol{y} - \hat{D}\boldsymbol{p}\right)^{\mathrm{t}}\left(\boldsymbol{y} - \hat{D}\boldsymbol{p}\right)\right] = 2\,\delta\boldsymbol{p}^{\mathrm{t}}\hat{D}\ \delta\boldsymbol{p} > 0. \tag{16}$$

Knowing the parameters B_i and C_i, the $z_i = \exp(-\Delta t/\tau_i)$ can then be found as the solutions of the polynomial

$$1 - \sum_{i=1}^{M} \frac{B_i}{z^i} = 0, \tag{17}$$

and the amplitudes A_i are given by

$$A_i = \sum_{j=0}^{M-1} \frac{C_j}{z_i^j} \Bigg/ \prod_{j\neq i}^{M}\left(1 - \frac{z_j}{z_i}\right). \tag{18}$$

But this approach does not take into account the statistical character of the measured data $\boldsymbol{y}$. Due to the noisiness of the data, Eq. (11) will take the more general form

$$\boldsymbol{y} = \hat{D}\boldsymbol{p} + \boldsymbol{e}, \tag{19}$$

where $\boldsymbol{e}$ is a random vector of residuals. What one can do is to estimate the best possible values for the $\boldsymbol{p}$ vector and predict from them the best $\boldsymbol{y}$ values,

$$\boldsymbol{y}_0 = \hat{D}\boldsymbol{p}_0, \tag{20}$$

where the subscript 0 stands for an estimated value. From this notation, we have

$$\boldsymbol{e} = \boldsymbol{y} - \boldsymbol{y}_0. \tag{21}$$

Let us now assume, that the covariance matrix of the vector $\boldsymbol{e}$ is known,

$$\mathrm{cov}(\boldsymbol{e}) = \langle (\boldsymbol{e} - \langle \boldsymbol{e} \rangle)(\boldsymbol{e} - \langle \boldsymbol{e} \rangle)^{\mathrm{t}} \rangle = \hat{V}, \tag{22}$$

where $\langle \boldsymbol{e} \rangle$ denotes the expectation value of $\boldsymbol{e}$. Thus, according to the central limit theorem [10], the residuals $\boldsymbol{e}$ have the approximate probability density distribution

$$P(\boldsymbol{e}) \propto \exp\left(-\tfrac{1}{2}\boldsymbol{e}'^{\mathrm{t}}\hat{V}^{-1}\boldsymbol{e}\right). \tag{23}$$

A maximum likelihood estimation of the parameters $\boldsymbol{p}$ (the most probably values of $\boldsymbol{p}$, see Ref. [11] and citations therein) will maximise the corresponding probability densitiy of the residuals $\boldsymbol{e}$, thus minimising the quadratic form

$$\boldsymbol{e}^{\mathrm{t}}\hat{V}^{-1}\boldsymbol{e} = \left(\boldsymbol{y} - \hat{D}\boldsymbol{p}\right)^{\mathrm{t}}\hat{V}^{-1}\left(\boldsymbol{y} - \hat{D}\boldsymbol{p}\right). \tag{24}$$

Therefore, one needs to know the covariance matrix of the residuals. Most frequently, the number of counts y_i in the ith channel will obey a Poissonian distribution with mean value $\langle y_i \rangle$ and mean deviation $\langle y_i^2 \rangle - \langle y_i \rangle^2 = \langle y_i \rangle$. Thus, the non-zero components of $\hat{V}$ are

$$V_{ij} = V_{ji}, \tag{25a}$$

$$V_{ii} = \langle y_{i+M} \rangle + \sum_{j=1}^{M} p_j^2 \langle y_{i-j+M} \rangle, \tag{25b}$$

$$V_{ij} = -p_{j-i}\langle y_{i+M} \rangle + \sum_{k=1}^{M-j+1} p_k p_{j-i+k} \langle y_{i-k+M} \rangle$$

$$\text{for } 1 \le j - i \le M. \tag{25c}$$

Here it was assumed, that the IRF is known exactly. In practise, this assumption is often acceptable since it is only a question of time to measure the IRF with arbitrary precision. But in general, it is straightforward to include also a Poissonian statistics of the IRF into Eqs. (25).

Minimising the quadratic form of Eq. (13) instead of Eq. (24) makes the resulting parameters $\boldsymbol{y}$ unpredictably sensitive to any noise in the measured data. To avoid this, Sasaki and Masuhara proposed a rather artificial way to reduce the noisiness of the data. Instead of solving directly Eq. (11), they applied a special filtering in Fourier space, $\hat{W}\hat{F}\boldsymbol{y} = \hat{W}\hat{F}\hat{D}\boldsymbol{p}$, where $\hat{F}$ is a discrete Fourier transform matrix and $\hat{W}$ is a diagonal weight matrix, the ith element of which is proportional to the second power of the ith element of the vector $\hat{F}\boldsymbol{y}$. Thus, their final solution for the parameter vector $\boldsymbol{p}$ reads

$$\boldsymbol{p} = \left[\left(\hat{W}\hat{F}\hat{D}\right)^{\mathrm{t}}\left(\hat{W}\hat{F}\hat{D}\right)\right]^{-1}\left(\hat{W}\hat{F}\hat{D}\right)^{\mathrm{t}}\hat{W}\hat{F}\boldsymbol{y}. \tag{26}$$

But this method of noise-reduction does only work for relatively simple cases (e.g. mono-exponential decay, low-noise data), but will often fail for complex decay patterns, as will be shown in the next section.

For the sake of completeness it should be mentioned, that neither the minimisation of Eq. (13) nor that of the more accurate expression Eq. (24) is equivalent to finding the minimum of the standard least-squares deviation minimum, which means minimising the quadratic form of Eq. (4).

In conclusion of this section some remarks concerning the practical application of Eq. (24) have to be added. The vector $\boldsymbol{p}$ which minimises the quadratic form Eq. (24) is given by

$$\boldsymbol{p} = \left(\hat{D}^{\mathrm{t}}\hat{V}^{-1}\hat{D}\right)^{-1}\hat{D}^{\mathrm{t}}\hat{V}^{-1}\boldsymbol{y}. \tag{27}$$

For employing this equation, one has to know the matrix $\hat{V}$, which itself depends on $\boldsymbol{p}$ and $\boldsymbol{y}$. A simple solution to this problem is to use approximate values for these variables to calculate $\hat{V}$. Taking into account, that in most practical cases the values of $\Delta t/\tau_i$ are much less than unity, and thus $\exp(-\Delta t/\tau_i) \approx 1$, the following approximations for the calculation of $\hat{V}$ are made:

$$p_1 \approx M, \tag{28a}$$

$$p_i \approx -\frac{M-i+1}{i} p_{i-1}, \tag{28b}$$

$$\langle y \rangle \approx y. \tag{28c}$$

3. Numerical simulations

Using the approximations of Eq. (28), we calculated the results of Eqs. (26) and (27) for different simulated data, and compared these results to the exact values (which entered the data simulation) and the values resulting from a least-squares fit. Moreover, we compared the least-squares fit with initial guess values taken from Eq. (27) with a similar fit, where the initial guess values were set equal to the exact values. Thus, one can test whether the values of the τ_i, A_i, resulting from Eq. (27), will give sufficient initial guess values for a subsequent non-linear least-squares minimisation. In all least-squares minimisations, a Nelder–Meade simplex algorithm [5] was used.

For the preparation of the computer-simulated data, the value of Δt was set to unity (thus defining the time unit). The instrumental response function was modelled by a Gaussian curve with full width at half maximum of 10, its maximum position in the 30th channel, and a peak height of 10^3 counts. The total number of sampling points was 256. In correspondence to real experiments, which make use of high-repetition solid-state lasers, we assumed a periodic repetition of the exciting laser pulse, whereas for simplicity the repetition period was also set equal to 256. The simulated data were fluctuated by a Poissonian noise, the mean standard deviation of which in the ith channel was equal to the exact value

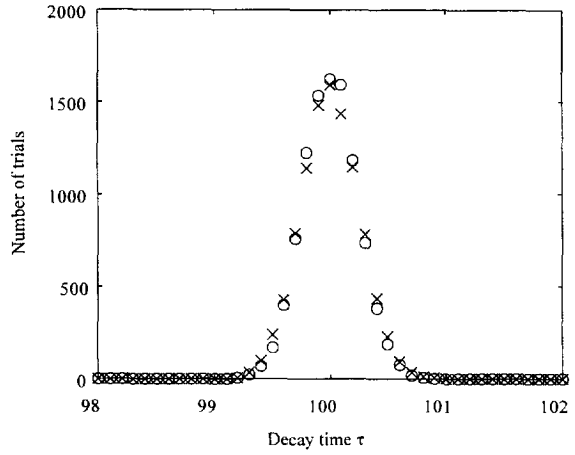

Fig. 1. Decay time distribution for 10^4 simulated mono-exponential decay data (amplitude $A = 1$, decay time $\tau = 100$) as calculated by Eq. (26) (crosses) and Eq. (27) (circles).

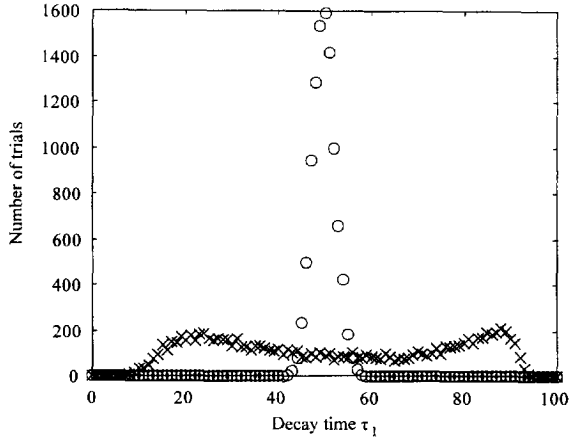

Fig. 2. Distribution of decay time τ_1 for 10^4 simulated bi-exponential decay data (amplitudes $A_1 = A_2 = 1$, decay times $\tau_1 = 50$, $\tau_2 = 150$) as calculated by Eq. (26) (crosses) and Eq. (27) (circles).

Table 1
Mean values and standard deviations of the parameter estimation for 10^4 simulated data curves

Exact	Eq. (26)		Eq. (27)	
	Mean value	Standard deviation	Mean value	Standard deviation
$A = 1$	1.0001	0.0066	1.0000	0.0025
$\tau = 100$	99.9995	0.2517	99.9990	0.2346
$A_1 = 1$	0.9985	0.4987	0.9967	0.0668
$A_2 = 1$	1.0125	0.3346	1.0039	0.0710
$\tau_1 = 50$	52.0256	25.3915	49.8023	2.4481
$\tau_2 = 150$	−222.00	2.67×10^4	149.9963	5.2766

Table 2
Fitting results for simulated monoexponential decay data

Exact		Eq. (26)			Eq. (27)			Least square fit		
A	τ	A	τ	χ^2	A	τ	χ^2	A	τ	χ^2
0.1	20	0.10	19.9	1.23	0.10	20.3	1.11	0.10	20.9	1.04
0.1	50	0.10	49.5	1.12	0.10	49.7	1.11	0.10	50.2	1.09
0.1	100	0.01	105.7	0.98	0.10	99.8	0.97	0.10	99.9	0.97
0.1	200	0.10	199.8	1.55	0.10	203.3	1.25	0.10	201.7	1.13
1.0	20	1.20	19.9	1.10	1.00	20.0	1.07	0.10	20.1	1.06
1.0	50	1.00	50.2	1.17	1.00	50.2	1.17	0.10	50.2	1.17
1.0	100	1.00	99.7	0.91	1.00	99.8	0.89	0.10	99.9	0.89
1.0	200	0.99	197.1	5.15	1.40	199.9	1.16	1.20	199.6	1.12

of the ith channel. The maximum count numbers of the final data were about 10^4.

In a first step, the parameter estimation was repeated for 10^4 simulated data sets for a mono-exponentially (amplitude $A = 1$, decay time $\tau = 100$) and for a bi-exponentially decaying system (amplitudes $A_1 = A_2 = 1$, decay times $\tau_1 = 50$, $\tau_2 = 150$). The mean values and standard deviations of the parameter estimations are summarised in Table 1, and decay time distributions of the different estimation methods are shown in Figs. 1–3. As can be seen, for the mono-exponential decay the method of Sasaki and Masuhara is nearly equivalent to the method presented here, but already for the bi-exponential decay, the situation changes significantly. Especially unexpected are the significantly wrong mean value and large standard deviation for τ_2 when using Eq. (26).

In a second step, a comparison with a non-linear least square minimisation for typical simulated decay curves were made, and the results are presented in Tables 2 and 3. Since the non-linear least-squares minimisation is a very time consuming calculation (up to 3 orders of magnitude longer than the method presented in this paper), it is not possible to perform a large number of trial estimations within a reasonable amount of computer time. Thus, only the results of the parameter estimation for one typical simulated

Table 3
Fitting results for simulated biexponential decay data

Exact		Eq. (26)			Eq. (27)			Least square fit		
A_1	τ_1	A_1	τ_1	χ^2	A_1	τ_1	χ^2	A_1	τ_1	χ^2
A_2	τ_2	A_2	τ_2		A_2	τ_2		A_2	τ_2	
1	50	0.03	4.40	1.76	0.32	38.90	1.02	1.22	52.17	1.00
1	70	1.97	60.28		1.69	63.94		0.78	72.50	
1	50	0.10	8.38	10.33	0.86	47.14	1.04	1.13	51.87	1.01
1	90	1.90	70.67		1.15	86.76		0.87	93.59	
1	50	0.23	11.21	110.46	1.06	51.98	1.37	1.05	52.12	1.07
1	150	1.71	100.62		0.93	153.49		0.94	153.82	
1	50	0.78	42.28	103.64	1.04	51.39	1.34	1.02	50.42	1.22
1	200	1.25	200.46		0.96	206.15		0.98	202.68	
1	50	−0.01	2.09	1.75	0.49	41.53	1.05	0.45	41.29	1.01
10	70	10.94	68.17		10.52	69.42		10.55	69.30	
1	50	0.13	8.35	15.75	0.71	43.39	1.10	0.60	40.79	1.00
10	90	11.09	87.86		10.31	89.33		10.41	88.91	
1	50	0.26	3.32	25.73	1.22	57.40	1.18	1.25	59.05	1.02
10	150	10.70	141.24		9.75	151.39		9.73	151.77	
1	50	0.31	6.79	65.62	0.94	52.71	1.02	1.10	58.53	1.02
10	200	10.59	186.50		10.04	199.18		9.87	201.05	

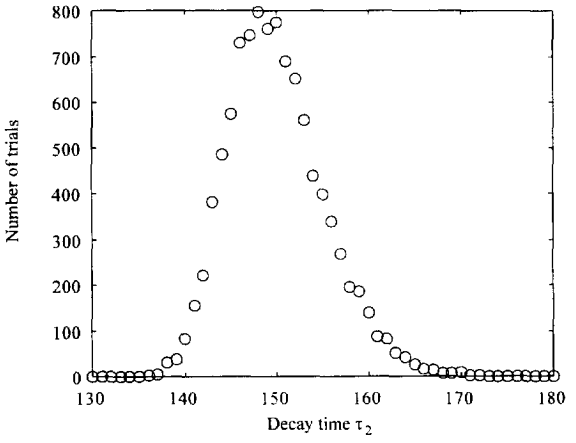

Fig. 3. Distribution of decay time τ_2 for 10^4 simulated bi-exponential decay data (amplitudes $A_1 = A_2 = 1$, decay times $\tau_1 = 50$, $\tau_2 = 150$) as calculated by Eq. (27). The results of Eq. (26) is not shown because of its extraordinarily broad distribution width (standard deviation $> 10^4$).

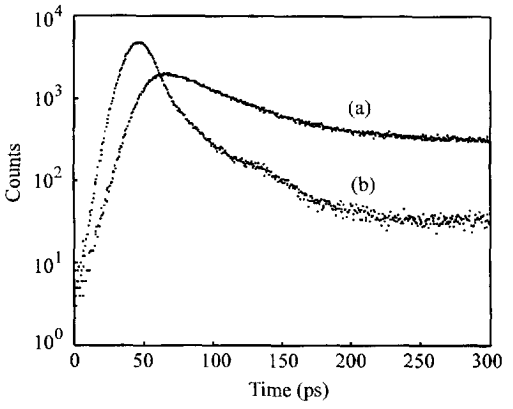

Fig. 4. (a) Fluorescence decay curve of a Porphyrine–Quinone in methylchloride; (b) instrumental response function.

data curve are given. Table 2 shows the results of the calculations for mono-exponential curves. As can be seen, Eq. (26) works not so bad in most cases. A not so desirable side effect is, that this equation yields almost always complex results, although with a small complex part compared with the real part. But in all cases, Eq. (27) gives better results, what underlines the effectiveness of the approximations of Eq. (28) for practical purposes.

In Table 3 the fit results for a bi-exponential decay are shown. In this case, again, the limitations of Eq. (26) can be clearly seen. In contrast, Eq. (27) works well in all cases.

4. Experimental data

We applied Eqs. (26) and (27) to the experimental measurement shown in Fig. 4. The curves there represent the fluorescence decay of a Porphyrine–Quinone [12] in methylene chloride and the instrumental response function. The excitation light source was an Ar^+-laser pumped and frequency doubled titan:sapphire laser, producing femtosecond pulses at 420 nm with 76 MHz repetition rate. The detector was a multichannel plate photomultiplier (Hamamatsu Photonics R 3809U), and the monochromator was a double grating type (Jobin–Yvon DHR-320). The electronics for time-correlated single-photon counting consists of a constant fraction discriminator (Tennelec), a time-to-amplitude converter (Tennelec), and a multichannel analyser (Ortec). To improve the time resolution, the electronics were additionally modified. The observed fluorescence wavelength was 650 nm. The instrumental response function was obtained by measuring the time profile of scattered light. Its full width at half maximum was less than 20 ps [13].

Measuring the instrumental response at the excitation wavelength of 420 nm, and the fluorescence at 650 nm, one cannot further neglect the differences in the instrumental response at different wavelengths (so called colour shift) [3]. Thus, as an additional fit parameter, one has to introduce an unknown time shift δ between the real instrumental response function at 650 nm and the measured one at 420 nm. This becomes especially important, if one looks for short fluorescence decay times. Here also, for getting a

Table 4
Dependence of the χ^2-value for the results of Eq. (27) applied to the data of Fig. 4 at different color shifts

Color shift δ	6	7	8	9	10	11
χ^2	735.32	98.79	12.04	15.65	18.06	21.01

Table 5
Comparison between Eq. (27) and a least-square fit for the data shown in Fig. 4

	A_1	A_2	τ_1	τ_2	δ	χ^2
Eq. (27)	1.45×10^{-2}	9×10^{-4}	54.4	3535	8.0	12.04
Least-square fit	1.35×10^{-2}	11×10^{-4}	60.5	5230	4.6	1.30

good initial guess value for δ, Eq. (27) can be used. In Table 4 are shown the different values of the chi square deviation, Eq. (4), for the results of Eq. (27) calculated at different values δ of the time shift.

Since the numerical calculation of Eq. (27) is very fast, it is no problem to screen several values of δ. As initial guess value for the subsequent least-squares minimisation one simply takes that time shift, which yields the minimum in Table 4. In Table 5 a comparison is made between the results of Eq. (27) and the least-squares minimisation. As can be seen, the results of Eq. (27) are in excellent vicinity to the value found by the least-squares fit.

5. Conclusion

In the present paper it was shown, that a modified version of the fit method independently proposed by Sasaki and Masuhara and by Apanasovich and Novikov gives excellent parameter estimations for multi-exponential fits of fluorescence decay curves. In perspective, the direct and numerically fast character of the method makes it ideally suited for estimating the optimal number of fit parameters (decay times) by examining, how the error function, defined by Eq. (24), changes for different numbers of fit parameters [14]. A similar application was demonstrated by the estimation of the colour shift in the last section. Thus, complex multi-exponential data fits are optimised and can be drastically reduced in computation time.

References

[1] J.R. Lakowicz, Principles of Fluorescence Spectroscopy (Plenum Press, New York, 1983).
[2] Topics in Fluorescence Spectroscopy, Ed. J.R. Lakowicz (Plenum Press, New York, 1994).
[3] D.V. O'Connor and D. Phillips, Time-correlated Single Photon Counting (Academic Press, London, 1984).
[4] V.V. Apanasovich and E.G. Novikov, J. Appl. Spec. 56(4) (1992) 538.
[5] J.A. Nelder and R. Meade, Comput. J. 7 (1965) 308.
[6] K.A. Levenberg, Quart. Appl. Math. II(2) (1944) 164.
[7] D.W. Marquardt, SIAM 11(2) (1963) 431.
[8] K. Sasaki and H. Masuhara, Appl. Optics 30(8) (1991) 977.
[9] V.V. Apanasovich, E.G. Novikov, Proc. SPIE. 2388 (1995) 378.
[10] D.T. Gillespie, Am. J. Phys. 51(6) (1983) 520.
[11] G. Leclerc and J.J. Pireaux, J. Electron Spectr. Rel. Phen. 71 (1995) 141.
[12] J. Sobeck, A. Wiehe, J. Enderlein, R. Erdmann and H. Kurreck, Proc. SPIE 2388 (1995) 369.
[13] R. Erdmann, G. Kell, W. Becker and E. Klose, Proc. SPIE. 2136 (1994) 300.
[14] Z. Bajzer, T.M. Therneau, J.C. Sharp and F.G. Pendergast, Eur. Biophys. J. 20 (1991) 247.